Boundary Operation of 2-D Non-separable Oversampled Lapped Transforms

Kosuke FURUYA†, Shintaro HARA† and Shogo MURAMATSU‡
†Graduate School of Science and Technology, Niigata Univ.
E-mail: {furuya, harashin}@telecom0.eng.niigata-u.ac.jp
‡Dept. of Electrical and Electronic Eng., Facl. of Eng, Niigata Univ.
E-mail: shogo@eng.niigata-u.ac.jp

***Abstract*—This paper proposes a boundary operation technique of 2-D non-separable oversampled lapped transforms (NSOLT). The proposed technique is based on a lattice structure consisting of the 2-D separable block discrete cosine transform (DCT) and non-separable redundant support-extension processes. The atoms are allowed to be anisotropic with the oversampled, overlapping, symmetric, real-valued, and compact-support property. First, the blockwise implementation is developed so that the atoms can be locally controlled. The local control of atoms is shown to maintain perfect reconstruction. This property leads an atom termination (AT) technique as a boundary operation. The technique overcomes the drawback of NSOLT that the popular symmetric extension method is invalid. Through some experimental results, the significance of AT is verified.**

I. Introduction

Filter banks and transforms are essential components of signal processing and there are a wide variety of applications such as compression, communication, denoising, restoration and feature extraction. For example, discrete cosine transform (DCT) and discrete wavelet transform (DWT) are popularly used in image and video processing. DCT is adopted by JPEG, MPEG-2 and MPEG4/AVC, while DWT is adopted by JPEG2000 and used for digital cinema[2][3]. These transforms however, have a disadvantage in representing diagonal edges and textures due to the separability. From this background, development of image transforms involves non-separable construction for handling such diagonal structures[1], [4]-[7]. The oversampled (OS) property is important as well as the non-separable property. Let us assume a P-channel filter bank. We denote the p-th channel down- and up-sampling factors as $\mathbf{M}_p$. Then the sampling ratio of the p-th channel, M_p, is given by $M_p = |\det(\mathbf{M}_p)|$. The total sum of the reciprocals of $\{M_p\}_{p=0}^{P-1}$ that is, $\sum_{p=0}^{P-1} \frac{1}{M_p}$ is called redundancy $\mathcal{R}$. When $\mathcal{R} = 1$, the system is referred to as a critically sampled (CS) filter bank. The other case, $\mathcal{R} > 1$, is called an oversampled (OS) filter bank. Advantage of OS filter bank is its high degree of design freedom[4][5]. There is infinite combination of analysis and synthesis banks in the OS case, while a CS system has unique combination.

The authors proposed two-dimensional (2-D) non-separable linear-phase paraunitary filter banks (NS-LPPUFB) before[8]. The transform is capable of directional property. We especially refer to it as a directional lapped orthogonal transform (DirLOT)[9]. DirLOT is non-separable and can simultaneously have the overlapping, orthonormal and symmetric property. The transform, however, is non-redundant and there is a problem that the single DirLOT has capability of representing only one direction. Two simple ways are well known to construct OS filter banks from CS ones. One is a mixture construction of multiple CS systems, and the other is a non-subsampled, or shift-invariant, construction, which is realized by removing the downsamplers and upsamplers from a CS system[7][9]. Indeed, we adopted a mixture construction by using multiple DirLOTs to obtain a multi-directional OS system in [10]. The redundancy $\mathcal{R}$ is, however, restricted to be integer in these approaches. In particular, the non-subsampled approach tends to have high redundancy. The higher redundancy is, the larger the computation and memory consumption become. From the fact, lower redundancy is requested while maintaining preferable properties for image processing.

In order to make the redundancy flexible, the authors have proposed 2-D non-separable oversampled lapped transform (NSOLT) as a new transform[11][12]. The transform is non-separable and can simultaneously satisfy the oversampled, overlapping, tight-frame, symmetric, real-valued and compact support property. As well, NSOLT can have rational redundancy. NSOLT with redundancy less than two was shown to be superior or comparable to the popular non-subsampled Haar wavelet transform in terms of image restoration performance[11][12]. NSOLT can be constructed in a lattice structure framework that we developed by generalizing the technique shown in [8].

Managing the boundary is one of important issues in the image processing applications, in order to reduce the boundary distortion. Note that the symmetric extension method is no longer applicable to NSOLT unless the fourfold symmetry is imposed on every atoms[15]-[17]. Although the periodic extension (PE) method can take the place of the symmetric extension method, it has drawbacks of wrapping effects and global memory access requirement at the border. This paper adopts a different approach for NSOLT. In [13] and [14], we have proposed a basis termination (BT) technique for the CS case. In order to extend the BT technique to the OS case, we propose a new technique, that is, atom termination (AT) by generalizing the previous technique.

The proposed technique is shown to serve variability of atoms block by block without any violation of the perfect

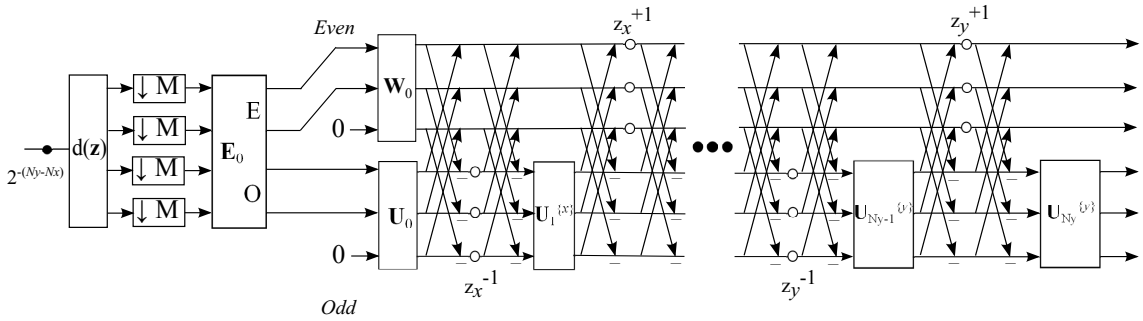

(a) Example of Type-I lattice structure of analysis NSOLT. (#Channel $P = 6$, Sampling factor $M = 4$)

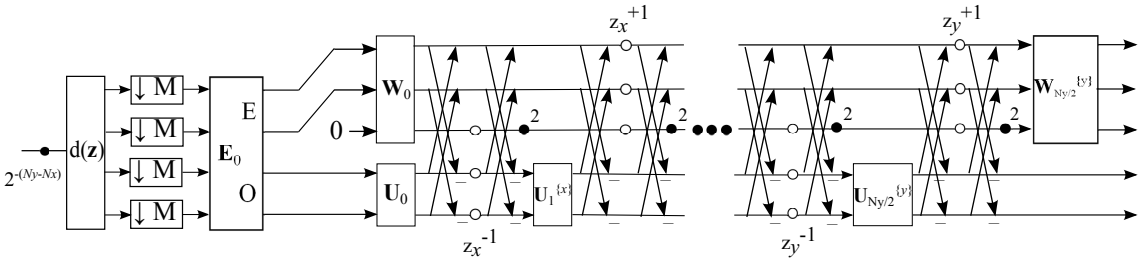

(b) Example of Type-II lattice structure of analysis NSOLT in $p_s > p_a$ case. (#Channel $P = 5$, Sampling factor $M = 4$)

Fig. 1. Type-I and Type-II lattice structure of analysis NSOLT, where $\mathbf{E}_0$ denotes symmetric orthonormal transform matrix directly given by 2-D DCT, and $\mathbf{W}_0$, $\mathbf{U}_0$, $\mathbf{U}_n^{\{d\}}$, $\mathbf{U}_\ell^{\{d\}}$ and $\mathbf{W}_\ell^{\{d\}}$ are arbitrary invertible matrices. N_d is the order of the polyphase matrix in the direction $d \in \{y, x\}$, and $\mathbf{d}(\mathbf{z})$ is the delay chain.

reconstruction. It is also shown that a special selection of the lattice parameters breaks off an overlapping relation between neighboring blocks locally. By applying this property at the border, we realize the atom termination.

This paper is organized as follows: in Section II, as a preliminary, the lattice structure of 2-D NSOLT is briefly reviewed. Section III derives the blockwise implementation technique for the lattice structure and the boundary operation with atom termination. Then, Section IV verifies the prospective significance of the proposed method through experimental results of non-linear approximation for diagonal texture image, followed by conclusions in Section V.

II. Review of 2-D nonseparable oversampled lapped transforms

NSOLT is a lattice structure realization of 2-D nonseparable oversampled linear-phase perfect reconstruction filter bank (NS OS LPPR FB). Let us review the lattice structure of NSOLT. First, we summarize some symbols and notations used throughout this paper.

M_y and M_x are reserved for decimation factors, respectively, in the vertical and horizontal directions such as

$$\mathbf{M} = \begin{pmatrix} M_y & 0 \\ 0 & M_x \end{pmatrix}.$$

Then, the total decimation factor is given by $M = |\det(\mathbf{M})| = M_y \times M_x$. As a preliminary, we define a $P \times P$ butterfly matrix $\mathbf{B}_P^{(m)}$ as

$$\mathbf{B}_P^{(m)} = \begin{cases} \frac{1}{\sqrt{2}} \begin{pmatrix} \mathbf{I}_m & \mathbf{I}_m \\ \mathbf{I}_m & \mathbf{I}_m \end{pmatrix} & , m = \frac{P}{2} \\ \frac{1}{\sqrt{2}} \begin{pmatrix} \mathbf{I}_m & \mathbf{O} & \mathbf{I}_m \\ \mathbf{O} & \sqrt{2}\mathbf{I}_{P-2m} & \mathbf{O} \\ \mathbf{I}_m & \mathbf{O} & \mathbf{I}_m \end{pmatrix}, & m < \frac{P}{2} \end{cases} \tag{1}$$

where $\lceil M/2 \rceil \le m \le \lfloor P/2 \rfloor$.

Through this paper, symbols $\mathbf{O}$ and $\mathbf{I}_m$ are reserved for the null and $m \times m$ identity matrix, respectively, where subscript m is omitted unless it is significant. A product of sequential matrices is denoted by $\Pi_{n=1}^{N} \mathbf{A}_n = \mathbf{A}_N \mathbf{A}_{N-1} \mathbf{A}_{N-2} \cdots \mathbf{A}_2 \mathbf{A}_1$.

A. Lattice Structure of 2-D NSOLT

In the article [8], we showed a method to construct multidimensional NS-LPPUFBs with a lattice structure, and then, in [18], Gan and Ma showed the reduced parameterization. NSOLT can simultaneously hold the oversampled, overlapped, symmetric, real-valued, and compact-support properties. It can also satisfy the paraunitary property and realize a Parseval tight-frame when the parameter matrices are restricted to be orthonormal. NSOLT is categolized into two types as:

- Type-I : $p_s = p_a$
- Type-II : $p_s \neq p_a$

where p_s and p_a denote the numbers of symmetric and antisymmetric atoms, respectively.

1) Type-I NSOLT: Fig. 1(a) shows an example of lattice structure of Type-I NSOLT. When the number of channels P is even, it is possible to set $p_s = p_a = P/2$. The polyphase

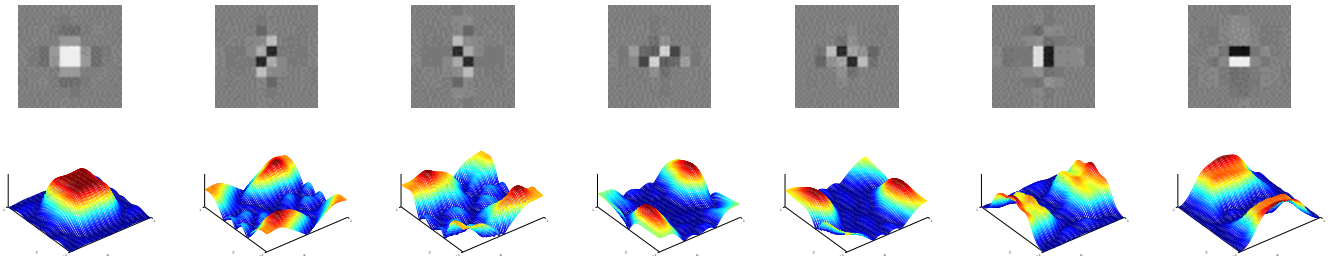

Fig. 2. Design example of Type-II NSOLT. The avobe figures are impulse response, and the under figures show frequency amplitude response, where $P = p_a + p_s = 7$, $M_y = M_x = 2(M = 4)$, $N_y = N_x = 4$.

matrix of Type-I has the following product form:

$$\mathbf{E}(\mathbf{z}) = \prod_{n_y=1}^{N_y} \{\mathbf{R}_{n_y}^{\{y\}} \mathbf{Q}(z_y)\} \prod_{n_x=1}^{N_x} \{\mathbf{R}_{n_x}^{\{x\}} \mathbf{Q}(z_x)\} \mathbf{R}_0 \mathbf{E}_0, \quad (2)$$

where

$$\mathbf{Q}(z_d) = \mathbf{B}_P^{(P/2)} \begin{pmatrix} \mathbf{I}_{p_s} & \mathbf{O} \\ \mathbf{O} & z_d^{-1}\mathbf{I}_{p_a} \end{pmatrix} \mathbf{B}_P^{(P/2)},$$

$$\mathbf{R}_n^{\{d\}} = \begin{pmatrix} \mathbf{I}_{p_s} & \mathbf{O} \\ \mathbf{O} & \mathbf{U}_n^{\{d\}} \end{pmatrix},$$

where $\mathbf{U}_n^{\{d\}} \in \mathbb{R}^{p_a \times p_a}$ is an arbitrary invertible matrix. We adopt the initial matrix $\mathbf{E}_0(\mathbf{z})$ defined by the product of the matrix representation of 2-D discrete cosine transform (DCT) $\mathbf{E}_0 \in \mathbb{R}^{M \times M}$ and

$$\mathbf{R}_0 = \begin{pmatrix} \mathbf{W}_0 & \mathbf{O} \\ \mathbf{O} & \mathbf{U}_0 \end{pmatrix} \begin{pmatrix} \mathbf{I}_{\lceil M/2 \rceil} & \mathbf{O} \\ \mathbf{O} & \mathbf{O} \\ \mathbf{O} & \mathbf{I}_{\lfloor M/2 \rfloor} \\ \mathbf{O} & \mathbf{O} \end{pmatrix} \in \mathbb{R}^{P \times M}, \quad (3)$$

that is, $\mathbf{E}_0(\mathbf{z}) = \mathbf{R}_0 \mathbf{E}_0$, where $\mathbf{W}_0 \in \mathbb{R}^{p_s \times p_s}$ and $\mathbf{U}_0 \in \mathbb{R}^{p_a \times p_a}$ are arbitrary invertible matrices. The analysis polyphase matrix $\mathbf{E}(\mathbf{z})$ in (2) satisfies

$$\mathbf{E}(\mathbf{z}) = \mathbf{z}^{-n} \mathbf{\Gamma}_P \mathbf{E}(\mathbf{z}^{-\mathbf{I}}) \mathbf{J}, \quad (4)$$

$$\mathbf{R}(\mathbf{z}) \mathbf{E}(\mathbf{z}) = \mathbf{z}^{-\overline{\mathbf{n}}} \mathbf{I}_M, \quad (5)$$

where $\mathbf{I}_M$ is the $M \times M$ identity matrix. The analysis polyphase matrix $\mathbf{E}(\mathbf{z})$ of (2) satisfies LP and PR.

2) Type-II NSOLT: Fig. 1(b) shows an example of lattice structure of Type-II NSOLT. Type-II NSOLT is given when $p_s \neq p_a$. We here consider only the case $p_s > p_a$ with even N_y and even N_x. The polyphase matrix $\mathbf{E}(\mathbf{z})$ of Type-II is represented by the following product form:

$$\begin{aligned} \mathbf{E}(\mathbf{z}) \quad = \quad & \prod_{\ell_y=1}^{\frac{N_y}{2}} \{\mathbf{R}_{E\ell_y}^{\{y\}} \mathbf{Q}_E(z_y) \mathbf{R}_{O\ell_y}^{\{y\}} \mathbf{Q}_O(z_y)\} \\ & \times \prod_{\ell_x=1}^{\frac{N_x}{2}} \{\mathbf{R}_{E\ell_x}^{\{x\}} \mathbf{Q}_E(z_x) \mathbf{R}_{O\ell_x}^{\{x\}} \mathbf{Q}_O(z_x)\} \mathbf{R}_0 \mathbf{E}_0, \quad (6) \end{aligned}$$

where

$$\mathbf{Q}_E(z_d) = \mathbf{B}_P^{(p_a)} \begin{pmatrix} \mathbf{I}_{P-p_a} & \mathbf{O} \\ \mathbf{O} & z_d^{-1}\mathbf{I}_{p_a} \end{pmatrix} \mathbf{B}_P^{(p_a)},$$

$$\mathbf{Q}_O(z_d) = \mathbf{B}_P^{(p_a)} \begin{pmatrix} \mathbf{I}_{p_a} & \mathbf{O} \\ \mathbf{O} & z_d^{-1}\mathbf{I}_{P-p_a} \end{pmatrix} \mathbf{B}_P^{(p_a)},$$

$$\mathbf{R}_{E\ell}^{\{d\}} = \begin{pmatrix} \mathbf{W}_\ell^{\{d\}} & \mathbf{O} \\ \mathbf{O} & \mathbf{I}_{p_a} \end{pmatrix}, \mathbf{R}_{O\ell}^{\{d\}} = \begin{pmatrix} \mathbf{I}_{p_a} & \mathbf{O} \\ \mathbf{O} & \mathbf{U}_\ell^{\{d\}} \end{pmatrix}.$$

$\mathbf{W}_\ell^{\{d\}} \in \mathbb{R}^{p_s \times p_s}$ and $\mathbf{U}_\ell^{\{d\}} \in \mathbb{R}^{p_a \times p_a}$ are arbitrary invertible matrices. We adopt the initial matrix $\mathbf{E}_0(\mathbf{z})$ defined by the product of the 2-D DCT $\mathbf{E}_0 \in \mathbb{R}^{M \times M}$ and $\mathbf{R}_0 \in \mathbb{R}^{P \times M}$ in (3). It can be verified that $\mathbf{E}(\mathbf{z})$ in (6). Type-II NSOLT also satisfies LP and PR as the same as Type-I NSOLT. Fig. 2 shows an example set of impulse responses and frequency amplitude responses[11][12]. Later, we use this design example in experiments.

B. Lattice Structure with Advance Shifters

When the transform is applied in the spatial domain, advance shifters are allowed. In order to realize these operations, we consider to modify $\mathbf{Q}(z_d)$ and $\mathbf{Q}_E(z_d)$ in each type of NSOLT.

1) Type-I NSOLT:

$$\overline{\mathbf{Q}}(z_d) = z_d \mathbf{Q}(z_d) = \mathbf{B}_P^{(P/2)} \begin{pmatrix} z_d \mathbf{I}_{p_s} & \mathbf{O} \\ \mathbf{O} & \mathbf{I}_{p_a} \end{pmatrix} \mathbf{B}_P^{(P/2)},$$

Then, we rewrite (2) for even N_y and N_x as

$$\begin{aligned} \mathbf{E}(\mathbf{z}) \quad = \quad & z_y^{-\frac{N_y}{2}} z_x^{-\frac{N_x}{2}} \prod_{n_y=1}^{N_y/2} \{\mathbf{R}_{2n_y}^{\{y\}} \overline{\mathbf{Q}}(z_y) \mathbf{R}_{2n_y-1}^{\{y\}} \mathbf{Q}(z_y)\} \\ & \times \prod_{n_x=1}^{N_x/2} \{\mathbf{R}_{2n_x}^{\{x\}} \overline{\mathbf{Q}}(z_x) \mathbf{R}_{2n_x-1}^{\{x\}} \mathbf{Q}(z_x)\} \mathbf{R}_0 \mathbf{E}_0. \quad (7) \end{aligned}$$

Fig. 1(a) show the lattice structure which corresponds to (7), where we omit to illustrate delays $z_y^{-\frac{N_y}{2}}$ and $z_x^{-\frac{N_x}{2}}$. Note that the operation with $\mathbf{Q}(z_d)$ is realized by the combination of the following matrices:

$$\mathbf{B}_P^{(P/2)} = \frac{1}{\sqrt{2}} \begin{pmatrix} \mathbf{I}_{P/2} & \mathbf{I}_{P/2} \\ \mathbf{I}_{P/2} & \mathbf{I}_{P/2} \end{pmatrix}, \mathbf{\Lambda}(z_d) = \begin{pmatrix} \mathbf{I}_{p_s} & \mathbf{O} \\ \mathbf{O} & z_d^{-1}\mathbf{I}_{p_a} \end{pmatrix}$$

as $\mathbf{Q}(z_d) = \frac{1}{2}\mathbf{B}_P^{(P/2)}\mathbf{\Lambda}(z_d)\mathbf{B}_P^{(P/2)}$. Then, the operation with $\overline{\mathbf{Q}}(z_d)$ is realized by $\mathbf{B}_P^{(P/2)}$ and

$$\overline{\mathbf{\Lambda}}(z_d) = \begin{pmatrix} z_d\mathbf{I}_{p_s} & \mathbf{O} \\ \mathbf{O} & \mathbf{I}_{p_a} \end{pmatrix}.$$

as $\overline{\mathbf{Q}}(z_d) = \frac{1}{2}\mathbf{B}_P^{(P/2)}\overline{\mathbf{\Lambda}}(z_d)\mathbf{B}_P^{(P/2)}$.

2) Type-II NSOLT: Similarly, by using the advance shifters Type-II NSOLT is realized by operator

$$\overline{\mathbf{Q}}_E(z_d) = z_d\mathbf{Q}_E(z_d) = \frac{1}{2}\mathbf{B}_P^{(p_a)}\begin{pmatrix} z_d\mathbf{I}_{P-p_a} & \mathbf{O} \\ \mathbf{O} & \mathbf{I}_{p_a} \end{pmatrix}\mathbf{B}_P^{(p_a)}.$$

Then, we can rewrite (6) for even N_y and N_x as

$$\begin{aligned}\mathbf{E}(\mathbf{z}) \quad = \quad & z_y^{-\frac{N_y}{2}} z_x^{-\frac{N_x}{2}} \prod_{\ell_y=1}^{N_y/2} \{\mathbf{R}_{E\ell_y}^{\{y\}}\overline{\mathbf{Q}}_E(z_y)\mathbf{R}_{O\ell_y}^{\{y\}}\mathbf{Q}_O(z_y)\} \\ & \times \prod_{\ell_x=1}^{N_x/2} \{\mathbf{R}_{E\ell_x}^{\{x\}}\overline{\mathbf{Q}}_E(z_x)\mathbf{R}_{O\ell_x}^{\{x\}}\mathbf{Q}_O(z_x)\}\mathbf{R}_0\mathbf{E}_0. \quad (8)\end{aligned}$$

Fig. 1(b) illustrates the lattice structure for (8), where we omit to draw the delays $z_y^{-\frac{N_y}{2}}$ and $z_x^{-\frac{N_x}{2}}$. Here, note that $\mathbf{Q}_E(z_d)$ is realized by the combination of the following matrices:

$$\mathbf{B}_P^{(p_a)} = \frac{1}{\sqrt{2}}\begin{pmatrix} \mathbf{I}_{p_a} & \mathbf{O} & \mathbf{I}_{p_a} \\ \mathbf{O} & \sqrt{2}\mathbf{I}_{P-2p_a} & \mathbf{O} \\ \mathbf{I}_{p_a} & \mathbf{O} & \mathbf{I}_{p_a} \end{pmatrix},$$

$$\mathbf{\Lambda}(z_d) = \begin{pmatrix} \mathbf{I}_{P-p_a} & \mathbf{O} \\ \mathbf{O} & z_d^{-1}\mathbf{I}_{p_a} \end{pmatrix},$$

as $\mathbf{Q}_E(z_d) = \frac{1}{2}\mathbf{B}_P^{(p_a)}\mathbf{\Lambda}(z_d)\mathbf{B}_P^{(p_a)}$. In addition, $\overline{\mathbf{Q}}_E(z_d)$ is realized by $\mathbf{B}_P^{(p_a)}$ and

$$\overline{\mathbf{\Lambda}}(z_d) = \begin{pmatrix} z_d\mathbf{I}_{P-p_a} & \mathbf{O} \\ \mathbf{O} & \mathbf{I}_{p_a} \end{pmatrix},$$

that is, $\overline{\mathbf{Q}}_E(z_d) = \frac{1}{2}\mathbf{B}_P^{(p_a)}\overline{\mathbf{\Lambda}}(z_d)\mathbf{B}_P^{(p_a)}$.

III. Boundary Operation

In this section, we propose blockwise implementation of NSOLT based on the lattice structure, and show the boundary operation for atom termination. Note that we describe them for Type-II NSOLT mainly because the way of the primitive block operations and the boundary operation for Type-II NSOLT are different from the previous work in [13]. In contrast, these operations for Type-I NSOLT are almost the same with [13] so that we omit to show the details of primitive block operations and the boundary operation for Type-I NSOLT.

A. Primitive Block Operations

1) Type-I NSOLT: The primitive block operation for Type-I NSOLT is realized by using the operations in Fig. 3. These operations are detailed in next paragraph section. Note that the center block vanishes block operations for Type-I NSOLT.

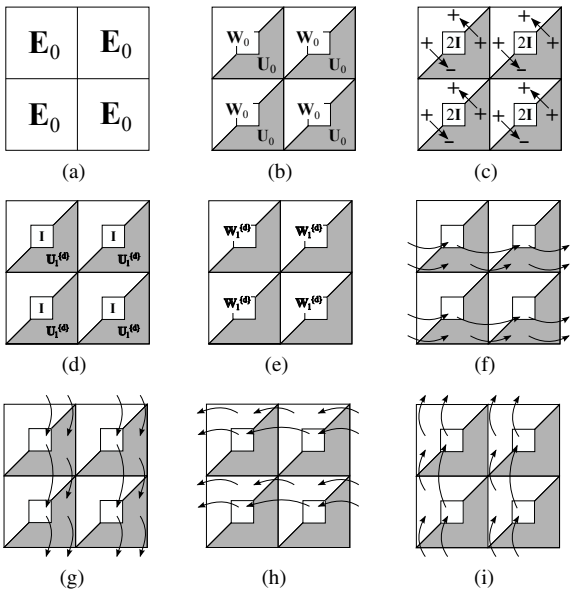

Fig. 3. Primitive block operations for Type-II NSOLT, where the white and shaded region mean operations for upper and lower half intermediate coefficient vectors, respectively, where $\mathbf{I}$ in the center block is the identity matrix for center intermediate coefficient. (a) $\mathbf{E}_0$, (b) $\mathbf{R}_0$, (c) $\mathbf{B}_P^{(p_a)}$, (d) $\mathbf{R}_{O\ell}^{\{d\}}$, (e) $\mathbf{R}_{E\ell}^{\{d\}}$, (f) $\mathbf{\Lambda}(z_x)$ (g) $\mathbf{\Lambda}(z_y)$, (h) $\overline{\mathbf{\Lambda}}(z_x)$ and (i) $\overline{\mathbf{\Lambda}}(z_y)$.

2) Type-II NSOLT: Fig. 3 summarizes the primitive block operations required for analyzing an image based on the product of (8), where 2×2 neighboring blocks are illustrated. Combination of these primitive operations can implement the analysis process, as in Fig. 1(b). Because the synthesis process can be realized through the inverse primitive operations in reverse order, we omit to show the detail.

The first operation with delay chain $\mathbf{d}(\mathbf{z})$, downsampling by factor $\mathbf{M}(= M_y \times M_x)$, and the transform by matrix $\mathbf{E}_0$ in Fig. 1 are exactly the same as the 2-D block DCT, which is shown in Fig. 3(a). Note that operation (a) is adopted to the block before inserting the center block coefficient. After dividing the 2-D DCT coefficients into two sets according to the atom symmetry, that is, even or odd symmetry, the transform with matrix $\mathbf{R}_0$ is applied as in Fig. 3(b), where the white and shaded region except the center block show operations for intermediate coefficients analyzed by the even- and odd-symmetric 2-D DCT basis images.

Next, Fig. 3(c) shows the operation with $\mathbf{B}_P^{(p_a)}$. This is nothing but the butterfly calculation. Fig. 3(d) illustrates the transform corresponds to matrix $\mathbf{R}_{O\ell}^{\{d\}}$ that processes only the lower half intermediate coefficients through matrix $\mathbf{U}_\ell^{\{d\}}$. In Fig. 3(e), it is shown that the matrix $\mathbf{R}_{E\ell}^{\{d\}}$ is applied to the upper half intermediate coefficients including the center block through matrix $\mathbf{W}_\ell^{\{d\}}$. Operations $\mathbf{\Lambda}(z_x)$ and $\mathbf{\Lambda}(z_y)$ in Fig. 3(f) and (g) delay the lower half intermediate coefficients. $\mathbf{\Lambda}(z_x)$ borrows the coefficients from the left block. Similarly, $\mathbf{\Lambda}(z_y)$ shifts the left block coefficients from the upper block. Fig. 3(h) and (i) illustrate the operations of $\overline{\mathbf{\Lambda}}(z_x)$ and $\overline{\mathbf{\Lambda}}(z_y)$, which return the upper half coefficients to the left and upper

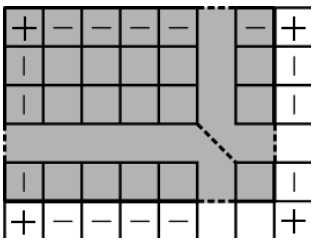

Fig. 4. Boundary operation using the block termination, where the shaded area denotes the original support region of a given image. The blocks including "|", "−" and "+" denote termination blocks in the horizontal, vertical, and both directions, respectively.

blocks, respectively. These primitive block operations are applied to every block in the order indicated by (8).

Note that all of the operations illustrated in Fig. 3(a)-(e) are independent of the other blocks. Although the delay and advance shift operations shown in Fig. 3(f)-(i) depend on the others, the relation is limited to the neighboring blocks. Therefore, the non-singular matrices $\mathbf{W}_0$, $\mathbf{U}_0$, $\mathbf{U}_\ell^{\{d\}}$ and $\mathbf{W}_\ell^{\{d\}}$ can vary block by block without any violation to the perfect reconstruction of the whole system.

B. Boundary Operation

The boundary treatment should be taken into account for some image processing applications since using the terminate operation for atoms can prevent distortion of boundary operation. Unfortunately, the popular symmetric extension approach is not available for NSOLT unless the fourfold symmetry is satisfied.

We propose to terminate the dependence between neighboring blocks by reducing the support region of atoms. Let us explain the relation to realize AT process in each type of NSOLT.

1) Type-I NSOLT: Type-I NSOLT AT can be achieved by the following relation for $\mathbf{U}_{2n-1}^{\{d\}}=-\mathbf{I}$:

$$
\begin{aligned}
&\overline{\mathbf{Q}}(z_d)\mathbf{R}_n^{\{d\}}\mathbf{Q}(z_d)\\
&=\mathbf{B}_P^{(P/2)}\begin{pmatrix} z_d\mathbf{I}_{p_s} & \mathbf{O}\\ \mathbf{O} & \mathbf{I}_{p_a}\end{pmatrix}\mathbf{B}_P^{(P/2)}\times\\
&\qquad\begin{pmatrix}\mathbf{I} & \mathbf{O}\\ \mathbf{O} & \mathbf{U}_n^{\{d\}}\end{pmatrix}\mathbf{B}_P^{(P/2)}\begin{pmatrix}\mathbf{I}_{p_s} & \mathbf{O}\\ \mathbf{O} & z_d^{-1}\mathbf{I}_{p_a}\end{pmatrix}\mathbf{B}_P^{(P/2)}\\
&=\frac{1}{4}\begin{pmatrix}(z_d+1)\mathbf{I} & (z_d-1)\mathbf{I}\\ (z_d-1)\mathbf{I} & (z_d+1)\mathbf{I}\end{pmatrix}\times\\
&\qquad\begin{pmatrix}\mathbf{I} & \mathbf{O}\\ \mathbf{O} & -\mathbf{I}\end{pmatrix}\begin{pmatrix}(1+z_d^{-1})\mathbf{I} & (1-z_d^{-1})\mathbf{I}\\ (1-z_d^{-1})\mathbf{I} & (1-z_d^{-1})\mathbf{I}\end{pmatrix}\\
&=\frac{1}{4}\begin{pmatrix}(z_d+1)\mathbf{I} & (1-z_d)\mathbf{I}\\ (z_d-1)\mathbf{I} & -(z_d+1)\mathbf{I}\end{pmatrix}\begin{pmatrix}(1+z_d^{-1})\mathbf{I} & (1-z_d^{-1})\mathbf{I}\\ (1-z_d^{-1})\mathbf{I} & (1-z_d^{-1})\mathbf{I}\end{pmatrix}\\
&=\frac{1}{4}\begin{pmatrix}4\mathbf{I} & \mathbf{O}\\ \mathbf{O} & -4\mathbf{I}\end{pmatrix}\\
&=\qquad\qquad\begin{pmatrix}\mathbf{I} & \mathbf{O}\\ \mathbf{O} & -\mathbf{I}\end{pmatrix}
\end{aligned}
\tag{9}
$$

where

$$
\mathbf{B}_P^{(P/2)}=\frac{1}{\sqrt{2}}\begin{pmatrix}\mathbf{I} & \mathbf{I}\\ \mathbf{I} & -\mathbf{I}\end{pmatrix},\mathbf{R}_n^{\{d\}}=\begin{pmatrix}\mathbf{I}_{p_s} & \mathbf{O}\\ \mathbf{O} & \mathbf{U}_n^{\{d\}}\end{pmatrix}.
$$

The equation (9) shows that the Type-I NSOLT can control the overlapping property of atoms. If the horizontal parameter matrices $\mathbf{U}_{2n-1}^{\{x\}}$ for all n in a block set to $-\mathbf{I}$, the relation of the current block to the left block is terminated. In addition, the vertical parameter matrices $\mathbf{U}_{2n-1}^{\{y\}}$ for all n in a block to $-\mathbf{I}$ terminates the relation of the current block to the upper block. This relation is equivalent to the basis termination (BT) in [13] because the number of upper and lower half intermediate coefficients are $p_s=p_a=\frac{P}{2}$. From this, Type-I NSOLT AT procedure is almost the same as the BT procedure so that we omit to show the detailed derivation of the AT for Type-I NSOLT. The Type-II NSOLT AT procedure is, however, different from Type-I NSOLT one. The difference appears in the implementation of Fig. 5(c) and (g) for coefficient shift processes. In the case of Type-I NSOLT, these processes are applied to only upper and lower half intermediate coefficients except the center block.

2) Type-II NSOLT: Type-II NSOLT AT can be realized as for $\mathbf{U}_\ell^{\{d\}}=-\mathbf{I}$

$$
\begin{aligned}
&\overline{\mathbf{Q}}_E(z_d)\mathbf{R}_{O\ell}^{\{d\}}\mathbf{Q}_O(z_d)\\
&=\mathbf{B}_P^{(p_a)}\begin{pmatrix} z_d\mathbf{I}_{P-p_a} & \mathbf{O}\\ \mathbf{O} & \mathbf{I}_{p_a}\end{pmatrix}\mathbf{B}_P^{(p_a)}\times\\
&\qquad\begin{pmatrix}\mathbf{I}_{p_a} & \mathbf{O}\\ \mathbf{O} & \mathbf{U}_\ell^{\{d\}}\end{pmatrix}\mathbf{B}_P^{(p_a)}\begin{pmatrix}\mathbf{I}_{p_a} & \mathbf{O}\\ \mathbf{O} & z_d^{-1}\mathbf{I}_{P-p_a}\end{pmatrix}\mathbf{B}_P^{(p_a)}\\
&=\frac{1}{4}\begin{pmatrix}(z_d+1)\mathbf{I}_{p_a} & \mathbf{O} & (1-z_d)\mathbf{I}_{p_a}\\ \mathbf{O} & 2z_d\mathbf{I}_{P-p_a} & \mathbf{O}\\ (z_d-1)\mathbf{I}_{p_a} & \mathbf{O} & -(z_d+1)\mathbf{I}_{p_a}\end{pmatrix}\times\\
&\qquad\begin{pmatrix}(1+z_d^{-1})\mathbf{I}_{p_a} & \mathbf{O} & (1-z_d^{-1})\mathbf{I}_{p_a}\\ \mathbf{O} & 2z_d\mathbf{I}_{P-p_a} & \mathbf{O}\\ (1-z_d^{-1})\mathbf{I}_{p_a} & \mathbf{O} & (1+z_d^{-1})\mathbf{I}_{p_a}\end{pmatrix}\\
&=\frac{1}{4}\begin{pmatrix}4\mathbf{I}_{P-p_a} & \mathbf{O}\\ \mathbf{O} & -4\mathbf{I}_{p_a}\end{pmatrix}\\
&=\qquad\qquad\begin{pmatrix}\mathbf{I}_{P-p_a} & \mathbf{O}\\ \mathbf{O} & -\mathbf{I}_{p_a}\end{pmatrix}
\end{aligned}
\tag{10}
$$

where

$$
\mathbf{B}_P^{(p_a)}=\frac{1}{\sqrt{2}}\begin{pmatrix}\mathbf{I}_{p_a} & \mathbf{O} & \mathbf{I}_{p_a}\\ \mathbf{O} & \sqrt{2}\mathbf{I}_{P-2m} & \mathbf{O}\\ \mathbf{I}_{p_a} & \mathbf{O} & \mathbf{I}_{p_a}\end{pmatrix},\mathbf{R}_{O\ell}^{\{d\}}=\begin{pmatrix}\mathbf{I}_{p_a} & \mathbf{O}\\ \mathbf{O} & \mathbf{U}_\ell^{\{d\}}\end{pmatrix}.
$$

From (10), Type-II NSOLT also can control the overlapping property of atoms. It is noticed that the relation in (10) reduces the number of overlapping blocks in direction $d\in\{y,x\}$. If the horizontal parameter matrices $\mathbf{U}_\ell^{\{x\}}$ for all ℓ in a block set to $-\mathbf{I}$, the relation of the current block to the left block is terminated. In addition, the vertical parameter matrices $\mathbf{U}_\ell^{\{y\}}$ for all ℓ in a block to $-\mathbf{I}$ terminates the relation of the current block to the upper block.

Fig. 4 illustrates the termination block position, where the blocks including "|", "−" and "+" denote the termination blocks in the horizontal, vertical and both directions. Around

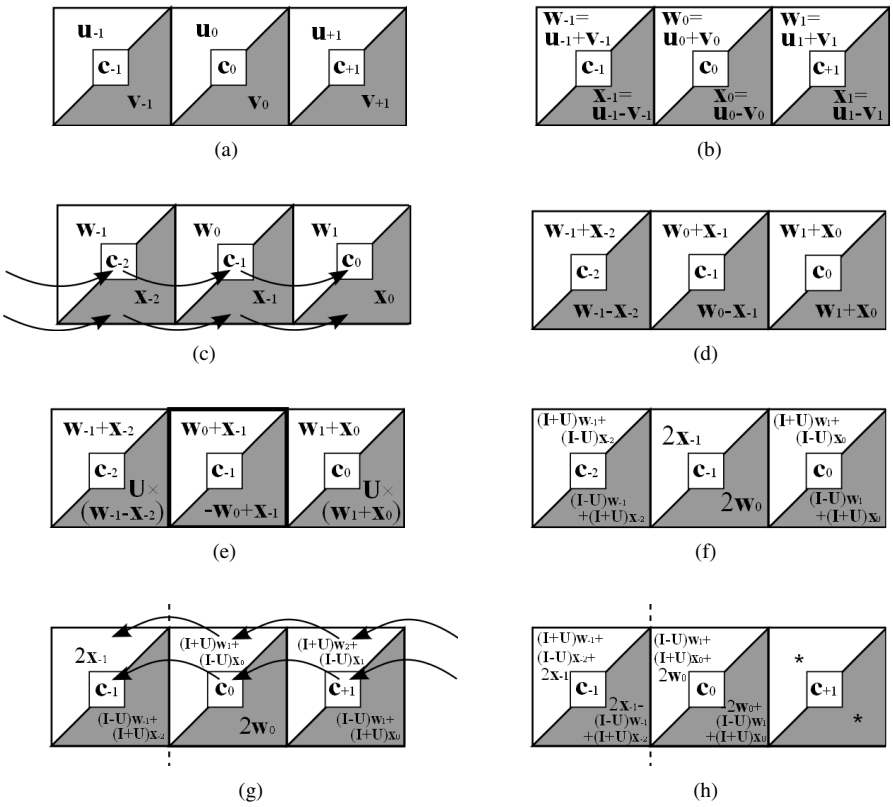

Fig. 5. Atom termination (AT) flow of the blockwise operations corresponding to (10), where succeeding three blocks are exemplified. (a) Intermediate coefficients of each blocks. (b) Operation with $\mathbf{B}_P^{(m)}$. (c) Operation with $\mathbf{\Lambda}(z_d)$. (d) Operation with $\mathbf{B}_P^{(m)}$. (e) Operation with $\mathbf{R}_{O\ell}^{\{d\}}$. (f) Operation with $\mathbf{B}_P^{(m)}$. (g) Operation with $\overline{\mathbf{\Lambda}}(z_x)$. (h) Operation with $\mathbf{B}_P^{(m)}$. These operations from (a) to (h) are applied alphabetical order, where $\mathbf{U}=\mathbf{U}_\ell^{\{d\}}$. In (e), the thick frame shows that the block to which parameter $\mathbf{U}_\ell^{\{d\}}=-\mathbf{I}$ is applied. The vertical dashed line in (g) and (h) denotes the separation of dependence between the blocks. For convenience, we omit to show the details in the right block in (h). Note that $\mathbf{c}_b$ in center block is operation of inserting 0 in Fig. 1.

the original picture, any value can be assumed since they have no influence on the essential transform coefficients.

Fig. 5 illustrates the local AT procedure in the blockwise operation in the case of Type-II NSOLT, where succeeding three blocks are denoted. Note that the discussion holds for both the horizontal and vertical directions.

In Fig. 5(a), $\mathbf{u}_b$ and $\mathbf{v}_b$ denote upper and lower intermediate coefficients, where b means the relative position from the current block. As well, the $\mathbf{c}_b$ in the center block contains a part of upper half intermediate coefficients vector. The next step is the butterfly operation with $\mathbf{B}_P^{(p_a)}$ for $\mathbf{u}_b$ and $\mathbf{v}_b$ block by block in Fig. 5(b), where $\mathbf{w}_b=\mathbf{u}_b+\mathbf{v}_b$ and $\mathbf{x}_b=\mathbf{u}_b-\mathbf{v}_b$. The butterfly operations are not adopted to $\mathbf{c}_b$. Then, each lower vector $\mathbf{x}_b$ and the center block $\mathbf{c}_b$ are moved to next block as shown in Fig. 5(c). After the operation Fig. 5(c), the butterfly operation is applied to vectors $\mathbf{u}_b$ and $\mathbf{v}_b$ again as in Fig. 5(d). In Fig. 5(e), the transform with $\mathbf{U}_\ell^{\{d\}}$ is applied to each lower vector, where we set $\mathbf{U}_\ell^{\{d\}}=-\mathbf{I}$ for the block of interest in the thick frame. After the butterfly operation in Fig. 5(f), each upper vector is advanced to the previous block, as shown in Fig. 5(g), and the butterfly operation is applied to as in Fig. 5(h).

Note that the left block of the vertical dashed line in Fig. 5(h) is independent of the coefficients for $b\geq 0$. Similarly, the right block is independent of the coefficients for $b<0$. These facts imply that these blocks have no relation to each other. That is, the atoms are terminated at the vertical dashed line without any violation to the perfect reconstruction.

IV. Experimental Result

Let us verify the significance of AT through the non-linear approximation performance. In this experiment, we use filters of three different extent, where polyphase order N_y and N_x set to $N_y=N_x=2,4$ and 6. Fig. 6 shows eight examples of the terminated atoms and one normal atom. It is observed that the region of support is properly controlled through the local termination process. These atoms are no longer symmetric at the border. However, they keep the PR and prevent the wrapping effect caused by the PE method. The difference between the normal image and terminated atoms is concentrated around the target boundary.

Fig. 7 shows experimental results of non-linear approximation in the order $N_y=N_x=4$. The original picture is given in Fig. 7(a), where the picture is in the 8-bit gray scale of size 128×128. Fig. 7(b) and (c) show the reconstruction results of the NSOLT with PE and the NSOLT with AT, respectively,

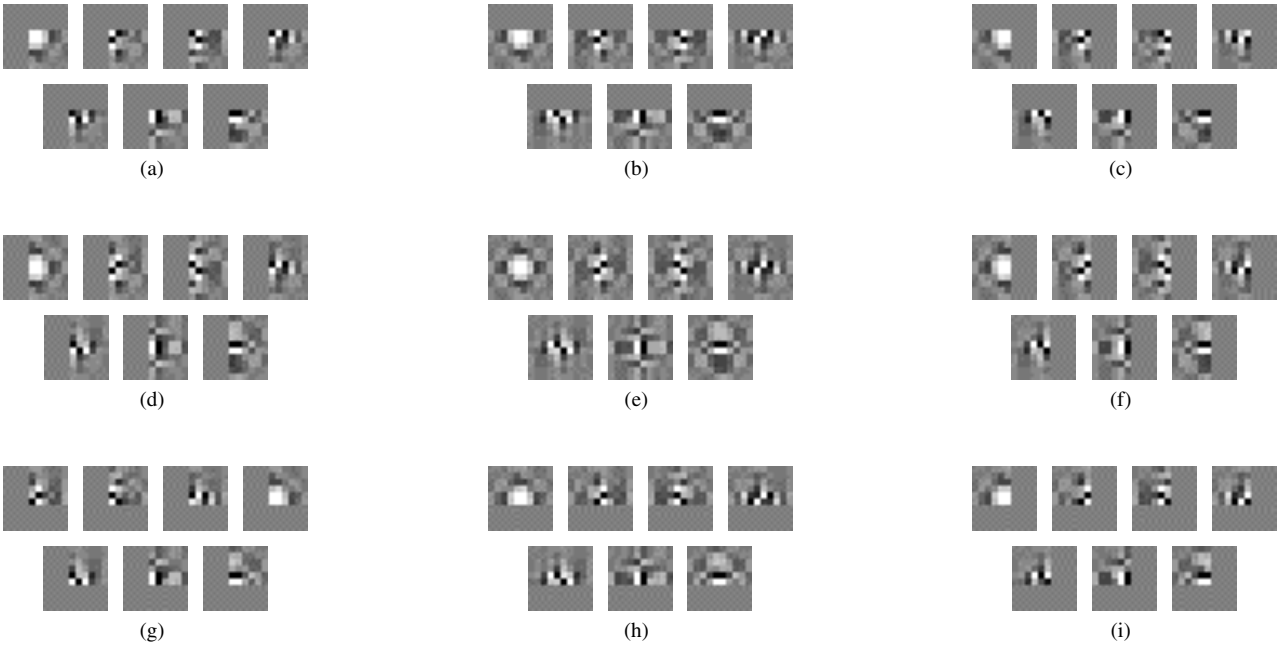

Fig. 6. These examples illustrate terminated atom images and the original normal atom image, and the contrast of each atom is enhanced in order to clarify the region of support. (a) Top left. (b) Top. (c) Top right. (d) Left. (e) Normal. (f) Right. (g) Bottom left. (h) Bottom. (i) Bottom right.

Fig. 7. Experimental results of non-linear approximation in $N_y = N_x = 4$, where (a) is an original picture part of Barbara in 8-bit gray scale of size 128×128, (b) and (c) show reconstruction results of the NSOLT with PE and AT, respectively. In the experiment, six-level hierarchical 2-D wavelet construction was adopted for all transforms and the number of transform coefficients in the non-linear approximation set to 500. (a) Original. (b) NSOLT with PE (PSNR: 21.15[dB]). (c) NSOLT with AT (PSNR: 21.44[dB]).

where the six-level hierarchical 2-D wavelet construction was adopted for each transform. The number of transform coefficients is set to 500 in non-linear approximation. From Fig. 7, it is observed that the PE method occurs wrapping effect at the bottom boundary. The AT method however, does not occurs the effect. Table-I shows peak signal-to-noise ratio (PSNR) for filters of different extent. From Table.I, NSOLT with AT gives a higher PSNR than that with PE in each case.

TABLE I
EXPERIMENTAL RESULT OF PSNR WITH PE AND AT.

Polypahse order	Periodic extension (PE)	Atom termination (AT)
2×2	21.15	**21.34**
4×4	21.15	**21.44**
6×6	21.25	**21.55**

V. CONCLUSION

In this work, we proposed a blockwise implementation of 2-D non-separable oversampled lapped transforms (NSOLT) and a boundary operation technique. This technique was shown to serve local variability of atoms without any violation of the perfect reconstruction. The blockwise implementation is effective for the image processing application since it allows us to control the region of support locally and leads a atom termination to prevent distortion at image boundary. Through experimental results, we verified the significance of the atom termination.

ACKNOWLEDGEMENT

This work was supported by KAKENHI (No.23560443).

REFERENCES

[1] M.Vetterli, "Wavelets, approximation, and compression," *IEEE Signal Process. Mag.*, vol. 18, No.5, pp. 59-73, Sep. 2001.

[2] K.R. Rao and P.C.L. Yip, eds., The Transform and Data Compression Handbook, Crc Pr I Llc, 2000.

[3] D. S. Taubman and M. W. Marcellin, "JPEG2000, image compression fundamentals, standards and practic", *Kluwer Academic Publishers*, 2002.

[4] S.Mallat, " A wavelet tour of signal processing," in *The Sparse Way*, 3rd ed. New York: Academic, 2008.

[5] Jelena Kovacevic and Amna Chebira, "Lofe beyond bases: The advent of frames (part i)," *IEEE Signal Process. Mag.*, vol.24, No.4, pp.86-104, 2007.

[6] M.N. Do and M. Vetterli, “The contourlet transform:An efficient directional multiresolution image representation” IEEE Trans. Image Process., vol.14, No.12, pp.2091-2106, Dec. 2005.

[7] J.-L. Starck, F.Murtagh, and J.M.Fadili, *Sparse Image and Signal Proessing: Wavelets, Curvelets, Morphological Diversity.* Cambridge, U.K.:Cambridge Univ. Press, 2010.

[8] S. Muramatsu, A. Yamada, H. Kiya, “A design method of multidemensional linear-phase paraunitary filter banks with a lattice structure,” *IEEE Trans. Signal Proc.*, vol. 47, No.3, pp. 690-700, March., 1999.

[9] S. Muramatsu, D. Han, T. Kobayashi, and H. Kikuchi, “Directional lapped orthogonal transform: Theory and design,” *IEEE Trans. Image Process.*, vol.21, No.5, pp.2434-2448, May 2012.

[10] S. Muramatsu, N. Aizaiwa, and M. Yukawa, “Image restoration with inion of directional orhonormal DWTs,” in *Proc. of APSIP ASC*, Dec. 2012.

[11] S. Muramatsu, N. Aizawa, “Lattice Structure for 2-D Non-separable Oversampled Lapped Transforms,” *Proc. IEEE ICASSP*, pp.5632-5636, May. 2013.

[12] S. Muramatsu, and N. Aizawa, “Image Restoration with 2-D Non-searapable Oversampled Lapped Transforms,” *Proc. IEEE ICIP*, Sep. 2013, to appear.

[13] S. Muramatsu, T. Kobayashi, M. Hiki, and H. Kikuchi, “Boundary operation of 2-D non-separable linear-phase paraunitary filter banks,” *IEEE Trans. Image Process.*, vol. 21, No. 4, pp. 2314-2318, Apr. 2012.

[14] S. Muramatsu and M. Hiki, “Block-wise implementation of directional GenLOT,” in *Proc. IEEE ICIP*, Nov. 2009, pp. 3977-3980.

[15] H. Kiya, K. Nishikawa, and M. Iwahashi, “A development of symmetric extension method for subband image coding,” *IEEE Trans. Image Process.*, vol. 3, No. 1, pp. 78-81, Jan. 1994.

[16] L. Chen, T. Q. Nguyen, and K.-P. Chan, “Symmetric extension methods for M-channel linear-phase perfect-reconstruction filter banks,” *IEEE Trans. Signal Process.*, vol. 43, No. 11, pp. 2505-2511, Nov. 1995.

[17] S. Muramatsu, A. Yamada, and H, Kiya, “The two-demensional lapped Hadamard transform,” *IEICE Trans. Fundam.*, vol. E81-A, No. 8, pp. 1542-1549, Aug. 1998.

[18] L. Gan and K.-K. Ma, “A simplified lattice factorization for linear-phase perfect reconstruction filter bank,” *IEEE Signal Process. Lett.*, vol. 8, No.7, pp 207-209, Jul. 2001.